Sl. No.	IIT Ropar List of Recent Publications with Abstract Coverage: September, 2021
1.	A Bi-Layer Clustered Priority Driven Energy Management Model for Inclining Block Rate Tariff Environment S Dash, R Sodhi, B Sodhi - IEEE Transactions on Industrial Informatics, 2021 **Abstract**: This paper proposes an energy management (EM) model for residences in an inclining block rate (IBR) tariff environment. Given a cluster, i.e., a group of appliances which satisfies certain requirements, the proposed scheme is primarily driven by two layers of clustered priorities. The first layer of clusters comprises various services of the residences and governs it with shareable z1 priorities, and the second layer of clusters binds the major power-consuming appliances under each substation and regulates it with dynamically changing z2 priorities. Integer linear programming is used to solve the multi-criteria decision problem crafted to address both grid-connected and isolated modes of operations. The model is tested on MATLAB using the IEEE 123-bus system with modified Pecan Street Dataset. Various results reveal that the proposed model is effective in providing a reliable power supply to the critical loads in all the scenarios while keeping the price within the preference limit with minimum comfort-loss for end-users, even in presence of non-responsive IBR environment.
2.	A biginelli-azophenol based robust sensor for rapid diagnosis of cyanide in real samples M Kaur, H Singh, N Kaur, N Singh - Dyes and Pigments, 2021 **Abstract**: The self-aggregation of multifunctional Biginelli-azophenol (Ligand1) in water (ONPs) led to sensitive and selective detection of toxic pollutant cyanide in an aqueous medium and solid matrix. The origin behind the excellent sensing performance of Ligand1 is assessed by 1H NMR spectroscopy which confirmed the deprotonation of OH and simultaneous H-bond formation by cyanide with NH of Ligand1. Furthermore, the UV–Visible absorption titration studies resulted in two isosbestic points at λ_{max} 399 nm and 314 nm, which also confirmed the complex formation between Ligand1 and CN^- with the detection of the lowest concentration of cyanide at 14.5 nM. Additionally, the colorimetric detection was supported by RGB color quantification as well as a thin column impregnated with Ligand1, which gives high-performance on-site cyanide detection in real water samples. Remarkably, such a cost-effective, robust colorimetric sensor having several key features, offered novel opportunities for real-time cyanide monitoring in polluted water and hence, this makes it unique among the other reported sensors for the same. **Graphical Abstract**: Multifunctional Biginelli-azophenol probe utilized to sensitively detect cyanide in an aqueous medium. A solid-matrix based thin column developed for rapid diagnosis of cyanide in an environmental polluted water samples by colorimetrically which is supported by RGB color quantification analysis. 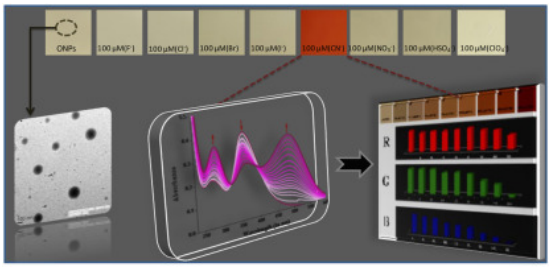

3.	A CMOS based High Resolution All-Digital Temperature Sensor with Low Power Supply Sensitivity S Das, S Wadhwa, DM Das - IEEE International Midwest Symposium on Circuits and Systems, 2021 **Abstract**: This paper presents the design of an All-Digital-Temperature Sensor (ADTS) with low power supply sensitivity (PSS). In this architecture, the delay cell-based ring-oscillator acts like a temperature sensor. The delay cells have been designed featuring the voltage compensation technique. This paper demonstrates the improvement over the conventional Current Starved Ring Oscillator (CSRO), and Voltage Compensated Ring Oscillator (VCRO) based temperature sensor. The proposed design consumes only 180µW power, exhibits PSS of 0.034°C/mV (i.e., 6-12%) and generates an error of only -0.4°C to +0.8°C across process comers and over the temperature range -40°C to 150°C and supply range of 1.8V +/-10%.
4.	A low power 8×2^{7}-1 PRBS generator using Exclusive-OR gate merged D flip-flops MK Singh, P Singh, DM Das, M Sakare - IEEE International Midwest Symposium on Circuits and Systems, 2021 **Abstract**: This paper presents an 8×2^{7} -1 pseudo-random binary sequence (PRBS) generator using Exclusive-OR (XOR) gate merged D flip-flops. In the proposed architecture, to ensure low power, a latch is removed from the D flip-flop and a dynamic logic based XOR gate along with a clock signal is used to get the functionality of master latch of the master-slave D flip-flop. In the proposed architecture of XOR gate merged D flip-flop, differential cascode voltage switch logic (DCVSL) XOR gate is selected from dynamic logic which provides a positive feedback (D-latch operation) in the pull-up network. The PRBS generator, which is designed using the proposed XOR gate merged D flip-flop, is designed in standard 65 nm CMOS technology. The post-layout simulation results confirmed the correct operation of the PRBS generator up to 2.56 Gb/s data rate with 1 V supply. The proposed architecture shows the best figure of merit compared to available PRBS generators in the literature to the best of the author's knowledge.
5.	A Machine Learning Pipeline for Measurement of Arterial Stiffness in A-Mode Ultrasound AK Sahani, D Srivastava, M Sivaprakasam, J Joseph - IEEE Transactions on Ultrasonics, Ferroelectrics, and Frequency Control, 2021 **Abstract**: Arterial stiffness (AS) of the carotid artery is an early marker of stratifying cardiovascular disease risk. This paper aims to improve performance of ARTSENS, a non-invasive A-mode ultrasound-based device for measuring AS. The primary objective of ARTSENS is to enable measurement of elastic modulus using A-Mode ultrasound and Blood pressure. As this device is image-free, there is a need to automate – a) carotid detection, b) wall localization and c) inner lumen diameter measurement. This has been performed using conventional signal processing methods in some of the earlier works in this domain. In this paper, deep neural network (DNN) models are employed to perform the above three tasks. The DNNs were trained over data acquired from 82 subjects at two different medical centers. Ground truth labeling was performed by a trained operator using corresponding measurements from state-of-the-art Aloka e-Tracking system. All three DNN models had significantly lower error compared to earlier signal processing methods and could perform their measurements using a single A-Mode frame. Using the DNNs, two different machine learning pipelines have been proposed here to measure the elastic modulus; best among them could achieve an error of 9.3% with Pearson correlation coefficient of 0.94 ($p < 0.001$). The models were tested on Raspberry Pi and Jetson Nano single board computers to demonstrate real-time processing on low computational resources.

6.	A Multi-path CNN for Automated Skin Lesion Segmentation J Chauhan, P Goyal – IEEE International Joint Conference on Neural Networks, 2021 **Abstract**: Automatic skin lesion segmentation in dermoscopic images is an essential requirement for making the computer-aided diagnosis (CADs) system, but efficiently segmenting skin lesions by using automated methods is not easy due to the factors such as color variations, illumination variations, presence of hair, etc. Researchers have recently been exploring deep convolutional neural networks (CNN) based methods in this domain. In this paper, we present a new and effective multi-path deep CNN method for automated skin lesion segmentation. The proposed network uses an encoder network in the first path and uses the learning representation from a pretrained base model's intermediate layers in its second path, for better learning of the features at different levels. Also, we use Instance Normalization that makes the network adaptive for each image and alleviates the problem that occurs due to different intensity images. Our method does not require any pre- or post-processing of the input dermoscopic images, except resizing in the beginning. The comparative performance evaluation of the proposed method is performed by considering two benchmark datasets: ISBI-2016 and ISBI-2017 and commonly used evaluation metrics including jaccard index and dice coefficient. The results analysis demonstrates the effectiveness of our approach, with our method achieving better performance in comparison to existing state-of-the-art methods overall and also on melanoma and non-melanoma images, across both the datasets.
7.	A novel μPMUs assisted loss-of-mains detection technique for active distribution systems Y Bansal, R Sodhi - Electric Power Systems Research, 2022 **Abstract**: In this paper, a novel Loss-of-Mains (LoM) detection scheme is proposed using the Adjoint Network principle with limited number of installed micro Phasor Measurement Units (PMU)s. The proposed scheme is comprised of two main stages viz., Off-line and On-line. In first stage, the network graph is divided into separate zones with two different Adjoints for each zonal area. The phasor information of the Adjoints are stored in matrices, as needed in the real-time process. The next step begins with Zonal Event Detection (ZED), which shrinks the LoM search area and ends up identifying the exact Point of Disconnection (PoD) using the Tellegen's Theorem in a ZED defined area. The major advantage of the suggested approach is that its reliability is independent of both the circumstances of the power mismatch and DG type. The efficacy of the proposed method is demonstrated through various simulated test cases and also, validated through Hardware-in-the-Loop (HIL) testing using Real-Time Digital Simulator (RTDS) and dSPACE1104 micro-controller on an unbalanced IEEE 13-bus distribution system integrated with PhotoVoltaic (PV) DGs.
8.	A numerical model for tool–chip friction in intermittent orthogonal machining A Saini, AD Jayal - Journal of Micromanufacturing, 2021 **Abstract**: This article presents a novel model to study the influence of surface textured cutting tools in near-micromachining conditions. The model utilizes the Challen and Oxley's asperity deformation model (Van Luttervelt et al., CIRP Ann Manuf Technol, 1998, vol. 47, pp. 587–626; Arrazola et al., CIRP Ann Manuf Technol, 2013, vol. 62, pp. 695–718) paired with an approach to a priori estimate of the interfacial film formation at the tool–chip interface. The procedure considers the chemical effect of the environment, along with the mechanical aspects of the surface texture of the cutting tool's rake surface. Model performance, in terms of predicting machining forces and coefficient of friction, was validated with existing experimental data (Anand et al., Proceedings of the international conference on advancements and futuristic trends in mechanical and materials engineering, 5–7 October 2012, pp. 661–666). The outcome trend of the proposed model approximately matches with the experimental results. Further, the model tries to explain the impact

	of cutting tool's surface roughness on overall tool–chip friction while performing intermittent cutting in the near-micromachining regime.
9.	A variational theory of zero field electronic specific heat of Anderson lattice model: An application to colossal magnetoresistive manganites (Re_{1-x} A_x MnO_3) S Panwar, I Singh - AIP Conference Proceedings, 2021 **Abstract**: Using a simple variational method, we have studied the zero field electronic specific heat (C_v) as a function of temperature of Anderson lattice model used for rare earth manganites doped with alkaline earths namely Re_{1-x} A_x MnO_3 (where Re=La, Pr, Nd etc., and A= Ca, Sr, Ba etc.) which exhibit colossal magnetoresistance (CMR), metal- insulator transition & many other poorly understood phenomena . We have already used this variational method to study the zero field electronic & magnetic properties like electrical resistivity & magnetic susceptibility of doped CMR manganites. We have taken two band (l-b) Anderson lattice model Hamiltonian for manganites in the strong electron- lattice Jahn- Teller (JT) coupling regime to study the temperature dependence of C v_{in} these compounds. We have also observed the role of the model parameters e.g. local Coulomb repulsion U, strong ferromagnetic Hund's Rule coupling J_H between e_g & t_{2g} spins & hybridization V_k between ℓ– polarons & d - electrons of the same spins on C_v & linear coefficient C_v/ T. We find from our results that as the temperature is lowered below a critical temperature T_c (~ 100 K), there is an anomaly (sharp peak) in both $C_v(T)$ &C_v/T beyond which it falls off for particular values of J_H, V & doping values x resembling with the key feature of many CMR compounds $La_{0.815}$ $Sr_{0.185}$ MnO_3 & $Pr_{0.6-x}Bi_xSr_{0.4}MnO_3$($x$ = 0.0- 0.15). The observed low temperature peak in $C_v(T)$ becomes progressively broader & shifts to higher temperature region on increasing V_k or J_H or doping x value. The specific heat anomaly near $T_c \sim 100$ K is related to magnetic ordering due to the paramagnetic- ferromagnetic transitions and magnetic inhomogeneity in these manganites.
10.	Advanced Finishing Processes for Biomedical Applications TS Bedi, R Kant, H Gurung - Advanced Micro- and Nano-manufacturing Technologies: Part of the Materials Horizons: From Nature to Nanomaterials book series, 2022 **Abstract**: Freeform surfaces have become an inevitable part of biomedical industries to carry out their specific task. Proper finishing of these surfaces is required to meet their high surface characteristics. The biomedical implants (made of biocompatible materials) such as shoulder, knee, ankle, finger, and hip joints require nanofinishing on the mating surfaces for their proper functionality and durability. The finishing of these implants is challenging because of their complex shapes and intricate features. Especially in conventional finishing processes, the rigid tool is used, which is mostly incapable of finishing the inaccessible areas of biomedical implants. Some advanced finishing processes have been developed which use flexible cutting tools to finish the freeform surfaces. These processes are suitable for micro/nanofinishing of biomedical components which enhance operational life as well as product value of the biomedical implants. This chapter discusses some of the advanced finishing processes, their applications, and advantages in biomedical industries.
11.	An Inverse Method for Parameter Retrieval in Solar Thermal Collector With a Single Glass Cover R Das - ASME Power Conference, 2021 **Abstract**: The present article highlights the implementation of differential evolution (DE)-assisted metaheuristic optimizer to provide the solution of an inverse multi-variable problem related to a flat absorber solar collector consisting of a single glass. For satisfying a given heating requirement from the solar collector, the necessary tilt angle and the thickness of the glass cover are simultaneously predicted using the proposed DE methodology. The existing study of inverse multi-variable

	optimization analysis has been done for dynamic values of solar energy radiation and different ambient conditions commonly encountered in various geographical locations of India. Formulation of the current research involves the minimization of a newly proposed cost function involving the required and the acquired heat transfer rates from the solar collector in Euclidean space. The solution approach then utilizes a dynamic exchange between evolutionary metaheuristic DE and a well-validated forward solver containing analytical expressions of heat energy balance within the solar collector. Variations of cost function and the estimated design variables are mainly studied to visualize the algorithm's behavior for a single gazing-based solar thermal device. Multiple possible groupings of the unknown parameters of the solar collector are revealed, which always collectively result in a desired heating requirement from the solar collector. Sensitivity indices related to the design variables are evaluated for ascertaining the relative importance of parameter selection. Encouraging opportunity is found towards the system's size reduction through sparing selection of inclination angle. The current study provides a convenient and cost-effective tool to select the necessary inclination and glass covers to obtain low to medium heating requirements from the available incident solar energy.
12.	Analysis of Parasitics on CMOS based Memristor Crossbar Array for Neuromorphic Systems SA Thomas, SK Vohra, R Kumar, R Sharma, DM Das - IEEE International Midwest Symposium on Circuits and Systems, 2021 **Abstract**: In this paper, a crossbar structure with CMOS based memristor emulator is presented where the spacing between the crossbar is modeled as per the memristor emulator circuit's area for a real-time design. The interconnect dimension in the crossbar structure corresponds to 180 nm CMOS technology, and the parasitics of the crossbar are extracted using ANSYS Q3D extractor. The extracted parasitic components are used to design a RC circuit model with the memristor emulator circuit to analyze the signal delay for different states of the memristor and crossbar sizes using the Cadence Virtuoso platform. The results of the crossbar architecture provide an insight into how the signal delay gets affected by the state of the memristor and with varying the load capacitance present at the memristor crossbar array's output.
13.	Analytical Model and PEA Experiment Based Study on Identification of Homocharge Conduction, Injection and Diffusion in LDPE AK Upadhyay, CC Reddy - IEEJ Transactions on Fundamentals and Materials, 2021 **Abstract**: Being an important member of polymeric insulation family, low density polyethylene is studied thoroughly. The major issue associated with it, homocharge accumulation (below 50 kV/mm), has got enough attention. Famous theories and simulation models have been put forth in regard to this. At the same time, available models ignored a well demonstrated concentration gradient of charges. According to the fundamental physics behind the concentration gradient of charges, the charges diffuse inside the material and contribute to the diffusion current. Available models/theories have only taken care of drift phenomenon of charges carriers, which is originated due to the electric field while neglecting the diffusion. Considering the gap, an analytical equation is derived after taking care of drift and the diffusion simultaneously. The analytical equation helps in identification and delineation of conduction of charges in bulk, diffusion of charge carriers and injection from the electrodes.
14.	Animacy modulates gender agreement comprehension in Hindi: An ERP study S Bhattamishra, R Muralikrishnan, KK Choudhary - Language, Cognition and Neuroscience, 2021 **Abstract**: The animate–inanimate distinction is of crucial importance cognitively, and animacy has been known to influence language comprehension. However, little is known about the role of animacy in verb agreement processing. The present study employed event-related brain potentials to

	examine whether the gender agreement of the verb with animate (natural gender) and inanimate (grammatical gender) subject nouns reveal similar or different processing mechanisms in Hindi. Critical stimuli were intransitive sentences of the form subject–verb–aux. Subject nouns were either animate or inanimate, and the verb either showed correct gender agreement or violated it. The violation of gender agreement with animate subjects evoked a P600 effect, whereas gender agreement violation with inanimate subjects revealed a long-latency N400-like effect. The result suggests that different underlying mechanisms are involved in the computation of gender agreement with animate and inanimate arguments in Hindi, illustrating the crucial role that animacy plays in verb agreement processing.
15.	Assessment of interstate dynamics of virtual water trade flows in primary crops production: Empirical evidence from India RR Chopra, SR Behera - Economics Bulletin, 2021 **Abstract**: This study examines the interstate virtual water trade flows embodied in wheat and rice products across India's different states and union territories during 1994â€“2017. Using the extended Leontief's input-output model, this study links the net virtual water trade flows with water scarcity concentration in Indian states. The input-output analyses decompose the water consumption into domestic demand and exports by the states. Empirical results show that the northern states have massive wheat and rice production, leading to the highest virtual water outflows to western and southern water-scarce states in India. Further, results exhibit that virtual water trade has substantial pressure on water-scarce states to become water-saving states. However, we find that water endowments, unsustainable water flows, and diversity lead to water scarcity concentration in water-abundant states.
16.	Assessment of performance, combustion and emissions characteristics of methanol-diesel dual-fuel compression ignition engine: A review MR Saxena, RK Maurya, P Mishra - Journal of Traffic and Transportation Engineering, 2021 **Abstract**: The energy security concern and rapidly diminishing fossil fuel resources demand the development of renewable and economically attractive fuel for reciprocating engines. Methanol is a promising renewable alternative fuel. Numerous studies have been carried out to explore the various aspects of the utilization of methanol in compression ignition (CI) engine. This review paper presents a detailed analysis of the effect of methanol on performance, combustion, and emission (NOx, CO, HC, and soot) characteristics of conventional CI-engine along with dual-fuel combustion mode. This study focuses on methanol utilization in dual-fuel mode, which is an advanced engine combustion mode. First, methanol production and solubility issues of methanol in diesel are briefly discussed. This study discusses the soot and nano-particle emission from the methanol fueled CI-engine, which is one of the main concerns in the current emission legislation. It was found that the utilization of methanol in CI-engine has the potential to improve the performance and simultaneously with a significant reduction in NOx, CO, soot, and nano-particle emissions in comparison to neat diesel operation. However, unburnt HC emission reduces for methanol-diesel blended fuel operation whereas HC emissions are higher for methanol-diesel dual-fuel operation.
17.	Bimodal Floquet theory of phase-modulated heteronuclear decoupling experiments in solid-state NMR spectroscopy R Garg, MK Pandey, R Ramachandran - The Journal of Chemical Physics, 2021 **Abstract**: A prescription based on bimodal Floquet theory is proposed to describe the nuances of phase-modulated supercycled decoupling experiments in solids. The frequency dependent interaction frames relevant to a particular supercycle are identified to facilitate faster convergence of perturbation corrections to the derived effective Hamiltonians. In contrast to silico-based methods,

	the proposed analytic method offers an attractive platform for faster optimization of experiments in solids. Additionally, the relevance of supercycling at ultrafast spinning conditions is also discussed.
18.	Can fingernail quality predict bone damage in Type 2 diabetes mellitus? a pilot study P Sihota, R Pal, RN Yadav, D Neradi, S Karn, VG Goni… V Mehandia…N Kumar… - PloS One, 2021 **Abstract**: Type 2 diabetes mellitus (T2DM) adversely affects the normal functioning, intrinsic material properties, and structural integrity of many tissues, including bone. It is well known that the clinical utility of areal bone mineral density (aBMD) is limited to assess bone strength in individuals with T2DM. Therefore, there is a need to explore new diagnostic techniques that can better assist and improve the accuracy of assessment of bone tissue quality. The present study investigated the link between bone and fingernail material/compositional properties in type 2 diabetes mellitus (T2DM). For that, femoral head and fingernail samples were obtained from twenty-five adult female patients (with/without T2DM) with fragility femoral neck fractures undergoing hemi/total hip arthroplasty. Cylindrical cores of trabecular bone were subjected to micro-CT, and lower bone volume fraction was observed in the diabetic group than the non-diabetic group due to fewer and thinner trabeculae in individuals with T2DM. The material and compositional properties of bone/fingernail were estimated using nanoindentation and Fourier Transform Infrared Spectroscopy, respectively. Both bone/fingernails in T2DM had lower reduced modulus (Er), hardness (H), lower Amide I and Amide II area ratio (protein content), higher sugar-to-matrix ratio, and relatively high carboxymethyl-lysine (CML) content compared with non-diabetic patients. Sugar-to-matrix ratio and relative CML content were strongly and positively correlated with HbA1c for both bone/fingernail. There was a positive correlation between bone and fingernail glycation content. Our findings provide evidence that the degradation pattern of bone and fingernail properties go hand-in-hand in individuals with T2DM. Hence, the fingernail compositional/material properties might serve as a non-invasive surrogate marker of bone quality in T2DM; however, further large-scale studies need to be undertaken.
19.	Catalyzing Bond-Dissociation in Graphene via Alkali-Iodide Molecules N Vats, DS Negi, D Singh, W Sigle, S Abb, S Sen…R Ahuja… - Small, 2021 **Abstract**: Atomic design of a 2D-material such as graphene can be substantially influenced by etching, deliberately induced in a transmission electron microscope. It is achieved primarily by overcoming the threshold energy for defect formation by controlling the kinetic energy and current density of the fast electrons. Recent studies have demonstrated that the presence of certain species of atoms can catalyze atomic bond dissociation processes under the electron beam by reducing their threshold energy. Most of the reported catalytic atom species are single atoms, which have strong interaction with single-layer graphene (SLG). Yet, no such behavior has been reported for molecular species. This work shows by experimentally comparing the interaction of alkali and halide species separately and conjointly with SLG, that in the presence of electron irradiation, etching of SLG is drastically enhanced by the simultaneous presence of alkali and iodine atoms. Density functional theory and first principles molecular dynamics calculations reveal that due to charge-transfer phenomena the C□C bonds weaken close to the alkali-iodide species, which increases the carbon displacement cross-section. This study ascribes pronounced etching activity observed in SLG to the catalytic behavior of the alkali-iodide species in the presence of electron irradiation.
20.	Chain-walking reactions of transition metals for remote C-H bond functionalization of olefinic substrates S Ghosh, S Patel, I Chatterjee - Chemical Communications, 2021 **Abstract**: Past several decades have witnessed the great evolution of inert C-H bond

	functionalization reactions as an emerging technique for synthesizing drug molecules, agrochemicals, and functional materials with intricate three-dimensional architectures. Although most activation of "unreactive" C-H bonds was accomplished by exploiting the power of transition metal catalysts, the distant and selective activation of unreactive C-H bonds in an undirected fashion remains one of the critical challenges to this rapidly growing field of organic chemistry. In this context, to meet all these concerns, much more attractive and challenging transition metal catalytic transformations have begun to blossom in recent years with the aid of the chain-walking process. The chain-walking strategy is one of the state-of-the-art techniques in organic synthesis to functionalize the unreactive C-H bonds by allowing the movement of a metal complex along the hydrocarbon chain of the substrate to recognize preferable bond-forming sites. The essential advantage of this strategy is that the bonds are formed only at the places where the catalyst selects for the specific C-H bonds to be cleaved, which not only avoids tedious synthetic procedures for prefunctionalization and the emission of undesirable wastes but also inspires chemists to plan novel synthetic strategies in a completely different manner. Consequently, various C-H bond functionalization reactions have been reported in recent years, employing the vast opportunity provided by this growing field mainly for the acyclic olefinic systems with flexible alkyl chains. Thus, chain-walking reactions allow the reactivity of the reaction centers within the substrates that cannot be realized via the classical mode of reactivity of the substrates. Applying this approach, inexpensive feedstock materials and simple hydrocarbons as an isomeric mixture can be converted to a single isomeric product in a regioconvergent scenario. Simultaneously, the site-selectivity of these reactions can also be switched using a regiodivergent strategy via appropriate tuning of ligands or a slight modification of reaction conditions. Herein, we have provided a comprehensive overview of the chain-walking reactions involving a variety of catalytic systems ranging from the first-row transition metal catalysts to the third-row transition metal catalysts for C-H activation in a concise fashion with the hope for further developments in this area through the appropriate application of the chain-walking reactions.
21.	Characterizing the tail behavior of daily precipitation probability distributions over India using the Obesity Index N Gupta, SR Chavan - International Journal of Climatology **Abstract**: Extreme precipitation events lie in the upper part of the probability distribution of daily precipitation data, i.e., the tail. Depending upon the tail behavior, various probability distributions are partitioned into heavy-tailed and light-tailed distributions. Heavy-tails tend to approach zero less rapidly than light-tails, signifying a higher frequency of occurrences for extreme precipitation events. Prediction of extreme precipitation depends on how reliably the distribution tail is modeled. Tail behavior can be studied by graphical as well as threshold-based fitting approaches. However, the graphical methods are time-consuming and do not provide quantitative comparisons between two distributions, whereas the threshold-based approaches possess limitations such as ambiguity in selecting an optimum threshold for demarcation of the tail. This paper assesses the utility of a simple empirical index, i.e., the “Obesity Index” to discern the probability distributions of daily gridded precipitation data with a resolution of 0.25° for historical (1951-2004) and future (2006-2099) periods over India into light- and heavy-tailed. The obesity index-based approach is an easy-to-use empirical approach that can quantitatively diagnose the heaviness of distribution tails without assuming any threshold for segregating the tails. Future projections of daily precipitation were obtained by downscaling simulations of the Coordinated Regional Climate Downscaling Experiment (CORDEX). Subsequently, a comparative analysis between the obesity index-based approach and threshold-based approaches by Nerantzaki and Papalexiou (2019) and Papalexiou et al. (2013) was conducted. Finally, the application of the obesity index-based approach is extended to characterize daily precipitation in Indian Meteorological Subdivisions. Further, we explored the dependence of

	the obesity index on the elevation of grids. Results indicated the applicability of heavy-tailed distributions in the representation of daily precipitation over India and suggest an obesity index-based approach as a good alternative diagnostic tool for assessing tail behavior.
22.	Coexisting commensurate and incommensurate charge ordered phases in CoO D Negi, D Singh, R Ahuja, PA van Aken - Scientific Reports, 2021 **Abstract**: The subtle interplay of strong electronic correlations in a distorted crystal lattice often leads to the evolution of novel emergent functionalities in the strongly correlated materials (SCM). Here, we unravel such unprecedented commensurate (COM) and incommensurate (ICOM) charge ordered (CO) phases at room temperature in a simple transition-metal mono-oxide, namely CoO. The electron diffraction pattern unveils a COM ($q1=1/2(1,1,1^{-})$ and ICOM ($q2=0.213(1,1,1^{-})$) periodic lattice distortion. Transmission electron microscopy (TEM) captures unidirectional and bidirectional stripe patterns of charge density modulations. The widespread phase singularities in the phase-field of the order parameter (OP) affirms the abundant topological disorder. Using, density functional theory (DFT) calculations, we demystify the underlying electronic mechanism. The DFT study shows that a cation disordering ($Co_1{-}x^{O}$,with x=4.17%) stabilizes Jahn-Teller (JT) distortion and localized aliovalent Co^{3+} states in CoO. Therefore, the lattice distortion accompanied with mixed valence states (Co^{3+},Co^{2+}) states introduces CO in CoO. Our findings offer an electronic paradigm to engineer CO to exploit the associated electronic functionalities in widely available transition-metal mono-oxides.
23.	Combustion of Hydrogen-Methane-Air-Mixtures in a Generic Triple Swirl Burner: Numerical Studies N Vishnoi, A Valera-Medina, A Saurabh, L Kabiraj - ASME Turbo Expo 2021: Turbomachinery Technical Conference and Exposition, 2021 **Abstract**: Ever-increasing energy demand, limited non-renewable resources, requirement for increased operational flexibility, and the need for reduction of pollutant emissions are the critical factors that drive the development of next generation fuel flexible gas turbine combustors. The use of hydrogen and hydrogen-rich fuels such as syngas helps in achieving decarbonisation. However, high temperatures and flame speeds associated with hydrogen might increase the NO_x emissions. Humidified combustion presents a promising approach for NO_x control. Humidification inhibits the formation of NO_x and also allows for operating on hydrogen and hydrogen-rich fuels. The challenge in the implementation of this technology is the combustor (burner) design, which must provide a stable combustion process at high hydrogen content and ultra-wet conditions. In the present work, we investigate the flow field and combustion characteristics of a generic triple swirl burner running on humidified and hydrogen enriched methane-air mixtures. The investigated burner consists of three co-axial co-rotating swirling passages: outer radial swirler stage, and two inner concentric axial swirler stages. Reynold's Averaged Navier-Stokes (RANS) simulation approach has been utilized here for flow description within the burner and inside the combustor. We present the flow fields from isothermal and lean pre-mixed methane-air reactive simulations based on the characterization of velocity profiles, streamwise shear layers, temperature fields and NO_x emissions. Subsequently, we investigate the effect of combustion on flow fields, and flame stabilization for hydrogen enriched methane-air mixtures as a function of hydrogen content. We also investigate the effect of humidified combustion on methane-hydrogen blends and present comparison of temperature estimations and NO_x emissions.
24.	Consumer Value Preferences in Healthcare: Insights for Value-centred Management S Saxena, Amritesh, SC Misra - Journal of Creating Value, 2021 **Abstract**: Advances in healthcare service research emphasize a value-driven approach in healthcare

	by pressing the need to acknowledge what matters to the patient against the conventional approach of what should be provisioned in the service. This research study adopts a consumer-centric perspective of value creation, and explores consumer value preferences in healthcare services, using netnography of online consumer reviews of cancer patients. Six different types of consumer value are identified, which carry varying consumer expectations. These are excellence, novelty, spirituality, ethics, privacy and control. The research findings confirm that all types of consumer values are not positive; rather, there is a presence of positive and negative (or must-be) elements. Privacy and ethics are identified as the negative or must-be type of consumer value, which creates not much satisfaction, but their absence is dissatisfying. Novelty and control are identified as positive value types whose absence may not be that problematic, but their enhancement creates greater customer satisfaction. The findings provide shreds of evidence to the claim that all value types are not positive, and consumers often make trade-offs between positive and negative value types while evaluating services. Future research is suggested in different healthcare contexts (e.g., chronic vs. non-chronic disease) to develop value-centred management strategies.
25.	Design, Modeling and Analysis of Cu-Carbon Hybrid Interconnects B Kumari, R Kumar, R Sharma, M Sahoo - IEEE Access, 2021 **Abstract**: In this work, a new interconnect structure is proposed for the first time where copper-carbon nanotube composite interconnect is encapsulated by graphene barrier layers named here as copper-carbon (Cu-carbon) hybrid interconnects. The motivation behind this new structure is to utilize the enhanced conductivity of copper-carbon nanotube (Cu-CNT) composite and improved reliability of copper-graphene (Cu-GNR) hybrid in order to build a better interconnect structure for possible replacement of copper interconnects in near future VLSI applications. The steps required to fabricate this structure is also proposed by utilizing the fabrication methods of Cu-CNT composite and Cu-GNR hybrid materials. First-principles-based atomistic simulations suggest that Cu-Carbon hybrid structure is more conductive than its parent structures, i.e. Cu-CNT composite and Cu-GNR hybrid. This deduction is also supported by the circuit simulation results at 7 nm node which show that Cu-Carbon hybrid interconnect experiences least delay among all other alternatives. When compared to Cu-GNR, Cu-CNT and Cu interconnects, delay in 1 mm long Cu-Carbon hybrid interconnect is lesser by ~28%, ~41% and ~88%, respectively. Time-domain analysis suggests that Cu-Carbon hybrid interconnect has the steepest and sharpest step response. Cu-Carbon hybrid interconnect has proven to be superior than other alternatives in terms of signal integrity. Noise-delay-product in a 1 mm long Cu-Carbon hybrid is lesser by ~42%, ~47% and ~84% as compared to Cu-GNR, Cu-CNT and Cu interconnects, respectively. Power consumption is also least in Cu-Carbon hybrid interconnects. Power-delay-product in a 1 mm long Cu-Carbon hybrid is also reduced by ~41%, ~44% and ~43% as compared to Cu-GNR, Cu-CNT and Cu interconnects, respectively. These findings promote Cu-Carbon hybrid interconnect as a superior candidate for near future VLSI applications.
26.	Design of a PRBS generator and a serializer using active inductor employed CML latch P Singh, MK Singh, VG Hande, M Sakare – IEEE International Midwest Symposium on Circuits and Systems, 2021 **Abstract**: This paper presents an inductor less D-latch for high-speed integrated circuits. The proposed D-latch uses negative feedback, which makes the high-frequency input impedance appear inductive. This effect increases the bandwidth by about 23%. The proposed latch operation is verified using two high-speed integrated circuit applications, i.e., A pseudo-random binary sequence (PRBS) generator and a serializer. The PRBS generator and the serializer show an improvement of 15.8% and 23%, respectively, using the proposed latch. Results are confirmed using post-layout simulation in standard 90 nm CMOS technology with 1 V supply.

27.

[Dexamethasone-loaded, Injectable Pullulan-Poly (ethylene glycol) Hydrogels for Bone Tissue Regeneration in Chronic Inflammatory Conditions]
N Chauhan, P Gupta, L Arora, D Pal, Y Singh - Materials Science and Engineering: C, 2021

Abstract: Chronic inflammation, infection, and fixation stability disrupts bone tissue regeneration by implants. The elevated levels of inflammatory markers and reactive oxygen species (ROS) damage tissues, inhibit osteoblastic differentiation, and promote bone resorption. Activation of local and chronic inflammatory responses due to the implantable biomaterial poses a high risk of implant failure and compromised bone repair in several pathological conditions. Not much progress has been made in the development of biomaterials that can counter inflammation and ROS along with inducing osteogenic activities for managing bone defects/injuries. We have developed, for the first time, injectable polymeric hydrogels by crosslinking oxidized pullulan (OP, 1% w/v) and 8-arm PEG hydrazine (PEG-HY, 10% w/v) using pH-sensitive and dynamic hydrazone linkages at 37 oC in buffer. The hydrogels were loaded with dexamethasone (Dex), an anti-inflammatory corticosteroid and osteogenic inducer, by covalently linking it to PEG-HY by hydrazone linkages, and their morphological, injectability, viscoelastic, self-healing, swelling, and drug-release properties were investigated. The hydrogels provided a pH-sensitive sustained release of PEG-Dex conjugate (3.62 wt%, 9.22 × 10-5 moles of Dex/gram) for 28 days, with 74.54 and 55.15% PEG-Dex conjugate being released at pH 6.5 and 7.4. ABTS assay showed that hydrogels inhibited 68% radicals within 1 hour, and treatment with hydrogel releasates inhibited the pro-inflammatory markers, IL-6 and IL-1β, and elevated the anti-inflammatory marker, TGF-β, in murine osteoblast precursor cells (MC3T3-E1). The hydrogels were found suitable for cell encapsulation and they exhibited 110% viability on treatment with releasates. Finally, the osteogenic activities of hydrogels were ascertained by alkaline phosphatase (ALP) activities, alizarin red S staining, and osteogenic gene expressions- RUNX2, Col-I, OPN, and IBSP. Overall, PEG-Dex conjugate released from hydrogels improved the cell viability and proliferation, and induced the osteoblastic differentiation. The hydrogels with their promising antioxidant and anti-inflammatory properties along with the osteogenic activities show a strong potential as an injectable, extracellular matrix (ECM)-mimicking implantable drug-depot for bone repair applications in chronic inflammatory conditions.

Graphical Abstract:

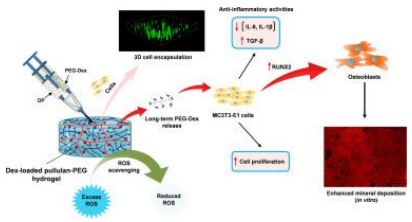

28.

[Dissociation of air pollutants on the uniform surface of pentagonal BeP2]
K Lakhani, S Kansara, SK Gupta, Y Sonvane…R Ahuja - Applied Surface Science, 2021

Abstract: In this present work, the investigation was carried out using density functional theory (DFT) for the dissociation of noxious gas molecules such as carbon and nitrogen-based molecules (CO, CO_2, N_2, NH_3, NO, and NO_2) on a pentagonal two-dimensional beryllium diphosphide (BeP2). The pentagonal BeP2 monolayer has a similar band structure as graphene. Here, some carbon and nitrogen-based noxious gases such as CO, CO_2, N_2, NH_3, NO, and NO_2 with Van der Waals (vdW) interaction behave like physisorbed, while strong covalent (Be-O) interactions of O_2 on BeP_2 formed chemisorption. Due to the chemisorption of O2 gas molecules, the bandgap at Dirac point at P-site on BeP_2 opens. While CO, CO_2, N_2, NO, and NO_2 are dissociated at the C-site, only CO, N_2, and

	NO are dissociated at the P-site. Beryllium diphosphide's band-gap shifts resulting from interactions with CO, N_2, and O_2 molecules are just 6%, 12.1%, and 22.2%, respectively, meaning that the BeP2 material has a moderate and high sensitivity towards CO, N_2, and O_2 molecules. BeP_2 appears to be a potential catalyst for the dissociation of CO, CO_2, N_2, NO, NO_2, and O_2 gas molecules, which is even more interesting.
29.	Diverse Receptive Field-based Adversarial Concurrent Encoder Network for Image Inpainting SS Phutke, S Murala - IEEE Signal Processing Letters, 2021 **Abstract**: Image inpainting is nowadays demanding because of its wide applications such as removing the unwanted objects from the image or recovering the old corrupted photo. Existing approaches achieved superior performance with coarse-to-fine or progressive or recurrent architectures for image inpainting regardless of computational complexity. In these types, the disturbance at the first instance or first iteration may lead to semantically unambiguous results. Also, to inpaint the image with varying hole sizes it is desirable to focus on the diverse receptive fields without deeper network i.e, network with less number of parameters. Therefore, we have proposed a lightweight adversarial concurrent encoder architecture with a diverse receptive field for image inpainting. Here, the concurrent encoder is integrated with diverse receptive fields to benefit with lower computational complexity. The proposed method is compared with state-of-the-art (SOTA) methods on Places2 and Paris Street View dataset in terms of peak signal-to-noise ratio and structural similarity index. Along with the extensive results analysis and ablation study, the proposed method proves the effectiveness in terms of less computational complexity compared to existing SOTA methods.
30.	Does the twin deficit hypothesis exist in India? Empirical evidence from an asymmetric non-linear cointegration approach L Mallick, SR Behera, RVR Murthy - The Journal of Economic Asymmetries, 2021 **Abstract**: This paper explores the dynamic relationship between the current account deficits and fiscal deficits in India. This paper has used the very much familiar Enders and Siklos (2001) and Hansen and Seo (2002) regime-switching threshold cointegration with an asymmetric error correction approach and non-linear ARDL model developed by Shin et al. (2014) to examine the non-linearity, short and long-run asymmetry, and asymmetrical adjustment between the current account deficits and fiscal deficits in India. Initial results validate the asymmetric adjustment between current account deficits and fiscal deficits, indicating the twin divergence hypothesis. However, the posterior sensitivity analysis suggests the twin deficit hypothesis, which seems more robust. Moreover, empirical results reveal that the interaction between these deficits is asymmetrically related, and fiscal deficits' upward and downward movement substantially affect India's current account deficits in the short-run and long run. The asymmetrical lead-lag relationship between current account deficits and fiscal deficits harms the current account sustainability, balance of payments, exchange rate, bond, and financial markets. Therefore, the study argues in its policy solution that the central bank of India must try to overcome the prolonged current account deficits and maintain stability in the domestic currency.
31.	Effect of local dissociation on symmetry breaking in exclusion model constituted by bridge lane and input-output TASEPs A Jindal, AK Gupta - Chaos, Solitons & Fractals, 2021 **Abstract**: Motivated by the dynamics of processive molecular motors in biological transport processes, we study the effect of local irreversible dissociation of two distinct species of particles moving along a bridge lane coupled to the input and output lanes governed by exclusion process. The boundary controlling rates of the particle in the bridge lane are determined self-consistently by

	the dynamics of the bridge and its feeding segments. A particle leaving the input lane is allowed to occasionally dissociate irreversibly from the exit site. The theoretical framework based on mean-field approximation is presented to understand how the local particle dissociations affect the bidirectional dynamics and spontaneous symmetry-breaking phenomena. Explicit phase boundaries and density profiles are obtained to analyse the steady-state behavior of the overall system. It has been observed that change in amplitude of dissociation rates leads to non-monotonic behavior of stationary phase diagrams and significant modifications in the dynamic properties. The emergence of new symmetric and asymmetric phases is reported under the symmetry of boundary controlling parameters and dissociation rates. Simple physical arguments are presented to explain the stationary properties of the system. Extensive Monte Carlo simulations are performed to test the validity of theoretical outcomes.
32.	Effect of Supporting Structure's Torsion on Floor Acceleration Demands in Buildings on Slopes A Jain, M Surana - Recent Advances in Earthquake Engineering: Part of the Lecture Notes in Civil Engineering book series, 2022 **Abstract**: A group of flat ground and step-back reinforced-concrete frame buildings are analysed to study their floor acceleration response. Bi-directional linear time history analyses are conducted in OpenSees using a suite of far-field seismic ground-motion records recommended in FEMA P695. Floor response spectra corresponding to the non-structural component's damping ratio of 5 % are obtained for the investigated buildings, in the direction along and across the slope, at two different storey levels. The floor acceleration response of these buildings is observed to be dominated by the fundamental mode at the roof level, whereas, by a higher mode, at the floor level immediately above the topmost foundation level. Further, this floor acceleration response of step-back buildings is observed to exhibit torsional amplification effects at the flexible edge, and de-amplification effects at the stiff edge, in the across-slope direction. This effect of torsional amplification is found to be maximum at the floor level immediately above the topmost foundation level. A correlation analysis of the torsional amplification factors with different torsional irregularity indices, i.e., the ratio of the maximum to minimum edge displacements, the ratio of the maximum to average edge displacements, floor rotation, and angular acceleration of the floor suggested that the torsional amplification factors are better correlated to the ratio between the maximum to minimum edge displacements, as compared to other investigated parameters.
33.	Electric Field-Modulated Charge Transfer in Geometrically Tailored MoX_2/WX_2 (X= S, Se) Heterostructures S Sahoo, MC Sahu, SK Mallik, NK Sharma, AK Jena…R Ahuja… - The Journal of Physical Chemistry C, 2021 **Abstract**: Light-induced interlayer charge transfer in staggered-type heterostructures (HSs) in transition-metal dichalcogenides provides the opportunity to improve the performance of optoelectronic applications. Herein, we employ density functional theory to investigate the vertical electric-field-controlled interlayer charge transfer in stacked MoX_2/WX_2 (X=S, Se) HSs. Upon application of electric field from −3 to 3 V/nm, we observe the band-alignment transition, band inversion, and offset variations in these HSs. Furthermore, these electric fields are found to modulate charge localization/delocalization across the layers, which provides insight into charge transfer. The positive electric field is supposed to localize the charges in WS2, whereas the charges are localized in MoS_2 at negative electric field. Based on charge localization/delocalization, our study suggests that the interlayer hole transfer upon MoS2 photoexcitation can be suppressed at higher positive electric fields, whereas electron transfer can be blocked by excitation of WS2. In contrast, negative electric fields (of −3 V/nm) can induce interlayer hole and electron transfer. Owing to the tunability of interlayer charge transfer by means of a vertical electric field, our

findings bear paramount importance in modulating electron–hole recombination and charge-transfer time, which is beneficial for future optoelectronic devices.

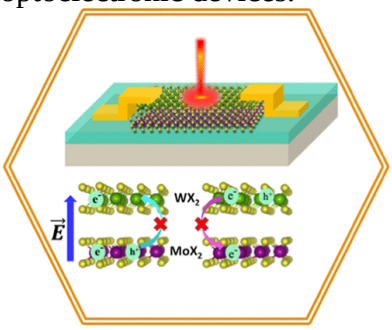

34. Electricity Driven 1, 3-oxohydroxylation of Donor-Acceptor Cyclopropanes: A Mild and Straightforward Access to β-hydroxy ketones
D Saha, IM Taily, P Banerjee - European Journal of Organic Chemistry, 2021

Abstract: An unprecedented external oxidant-free electrochemical protocol for 1, 3-oxohydroxylation of donor-acceptor cyclopropane is disclosed. The strategy encompasses the activation of the labile π-electron cloud of the aryl ring to cleave the strained C_{sp^3}–C_{sp^3} bond of cyclopropane to afford the *β*-hydroxy ketones via insertion of molecular oxygen. More significantly, based on the detailed mechanistic investigations and cyclic voltammetry experiments, a plausible mechanism is proposed.

35. Electronic, optical and thermoelectric properties of two-dimensional pentagonal SiGeC4 nanosheet for photovoltaic applications: First-principles calculations
I Bouziani, Z Haman, M Kibbou, I Essaoudi, A Ainane, R Ahuja - Superlattices and Microstructures, 2021

Abstract: In this theoretical study, based on the density functional theory, we investigate the electronic, optical and thermoelectric properties of SiGeC4 nanosheet, within the framework of mBJ-GGA approximation (modified Becke–Johnson generalized gradient approximation). The calculated results indicate that the two-dimensional SiGeC4 compound is energetically, dynamically, thermally and mechanically stable in the pentagonal structure and shows semiconductor character with indirect and moderate bandgap. Also, it is found that this two-dimensional system presents high absorption and low reflectivity as well as high photoconductivity in the visible range. Furthermore, it is shown that the studied compound exhibits good thermoelectric performance with high electrical conductivity and Seebeck coefficient. These results render the two-dimensional pentagonal SiGeC4 nanosheet as strong absorber layer candidate in the next generation of photovoltaic devices.

36. Energy consumption analysis of electrostatically assisted flat and tubular based filtration test rigs using polyester conductive media
S Dutta, A Mukhopadhyay, AK Choudhary, CC Reddy - Indian Journal of Fibre & & Textile Research, 2021

Abstract: In current study, the energy utilized by two types of laboratory based electrostatically assisted pulse jet filtration set-ups, viz. flat media test rig and tubular based test rig has been analyzed and compared. Three types of polyester nonwoven conductive filter media viz. polytetraflouroethylene coated media, stainless steel fibre blended with polyethylene terephthalate media and stainless steel scrim media have been characterized on both setups at three levels of aerosol charge, viz. 4 kV, 8 kV, 12 kV and without charge. The results reveal a significant drop in

	energy utilization ranging from 20% to 35% at pre-charge levels for both setups. Among all three materials, polytetraflouroethylene coated material is known to perform the best in both test setups. The contribution of compression energy in total power consumption is found to decrease in tubular based setup. However, the total energy consumption has been found to be the lower for flat media test rig.
37.	Energy Saving Assessment of Triple-Hybrid Vapor Absorption Building Cooling System Under Hot-Dry Climate G Singh, R Das - ASME Power Conference, 2021 **Abstract**: Thermally driven vapor absorption-based air-conditioning systems possess many advantages over the compression based systems. However, intermittent availability of input resources affects the operation of these absorption systems which causes discontinuous working. This study aims at examining the electrical and thermodynamic performance of a triple-hybrid vapor absorption-assisted air-conditioning system against a conventional system with the aid of EnergyPlus simulations for a small office building. The outside weather is subjected to hot-dry climatic condition. The heat input source includes biomass and solar energy-based resources. Auxiliary heat input is also used to ensure smooth operation. The performance of the absorption system is assessed at different generator temperature (70 °C–80 °C) and solar collector area (400 m^2–500 m^2). The results show that, by using absorption-based systems, a maximum of 34.1% electrical energy savings can be ensured at 500 m2 collector area with 70 °C generator temperature. The coefficient of performance of the absorption system escalates from 0.50 to 0.52 by increasing the generator temperature form 70 °C to 80 °C. Under the condition of 70 °C generator temperature and 500 m2 collector area, the absorption system can be made fully renewable energy dependent.
38.	Excited-State Intramolecular Hydrogen-Bonding-Assisted Restricted Rotation: A Mechanism for Monitoring Intracellular Viscosity and Distinguishing Malignant, Differentiating, and Apoptotic Cancer Cells Mayank, J Sindhu, A Singh, N Nayak, N Garg, N Kaur, N Singh - ACS Applied Bio Materials, 2021 **Abstract**: We have successfully developed a sensor (IP1) that utilizes a confocal-based live-cell imaging technique for distinguishing malignant, differentiating, and under-apoptosis cancer cells. The intracellular viscosity (IVis) is minimum in the cancer cell, intermediate in differentiating cells, and maximum in the apoptotic cells. Therefore, we have developed a molecular rotor (IP1) that can sense the changes in intracellular viscosity. IP1 works on the viscosity-assisted restricted-rotation mechanism and is facilitated by the excited-state intramolecular hydrogen-bonding phenomenon (ESIHB). The use of ESIHB has fine-tuned the viscosity-sensing properties of IP1, which in turn has greatly helped in our quest of distinguishing the malignant, differentiating, and apoptotic cancer cells by the IP1 probe. It was very effective in monitoring apoptosis by increased fluorescence intensity by the confocal live-cell imaging technique. The noncytotoxic behavior, even at 10 μg/mL concentration, is a charming feature of the developed probe. To the best of our knowledge, this is the first report for the ESIHB-based fluorescence probe that can distinguish malignant, differentiating, and apoptotic cancer cells by the use of live-cell imaging techniques.

	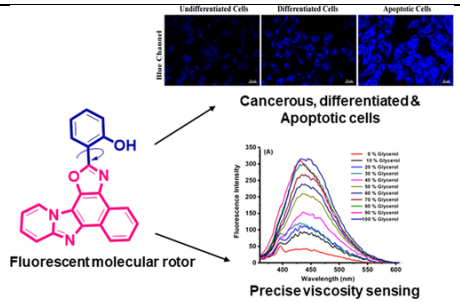
39.	Full CMOS Implementation of Bidirectional Associative Memory Neural Network with Analog Memristive Synapse SK Vohra, S Thomas, M Sakare, DM Das – IEEE International Midwest Symposium on Circuits and Systems, 2021 **Abstract**: Memristor is a computational and area efficient substitute for resistive synapse in neural networks as it provides tunable and non-volatile storage of synaptic weights. Full CMOS circuit realisation of a 6 × 6 Bidirectional Associative Memory (BAM) neural network with CMOS memristor synapse is implemented in this paper. To show the BAM neural network's ability to recall its pattern, we have taken the training set of three Tetris pattern pairs, and corresponding synapse weights are calculated using MATLAB. We have integrated the proposed tunable CMOS memristor emulator in the crossbar for storing the synaptic weights. The CMOS circuit implementation of the BAM neural network is validated with the simulation results in 0.18µm CMOS technology.
40.	Fusion of SCATSAT-1 and optical data for cloud-free imaging and its applications in classification S Singh, RK Tiwari, V Sood, S Prashar - Arabian Journal of Geosciences, 2021 **Abstract**: Earth observation via optical-based remote sensing is one of the effective solutions to cover the large swath and to deliver the very high-resolution dataset at the different wavelengths. But the applicability of optical imaging is limited by daytime only and adversely affected by the presence of clouds. In such scenarios, microwave data is more preferable due to the potential of penetrating through the clouds. Recently launched (26 September 2016) scatterometer satellite (SCATSAT-1) data by the Indian Space Research Organization (ISRO) has the potential of providing all-weather, day-night monitoring and daily data-delivery services at the global level. Along with the numerous advantages, the Ku-band (13.535 GHz) based SCATSAT-1 cannot provide sufficient information as provided by the multispectral optical sensors. Therefore, in the present work, the microwave-based SCATSAT-1 and optical-based MODIS (moderate resolution imaging spectroradiometer) have been fused using the nearest-neighbour approach to examine its effects in cloud removal and its applications in classification. The study has been performed over Himachal Pradesh, India. This study has also discussed the impact of different classifiers such as artificial neural network (ANN), spectral angle mapper (SAM), support vector machine (SVM), and random forest (RF), on the fusion of SCATSAT-1 (including backscattered coefficients, i.e. sigma-nought and gamma-nought at HH and VV polarizations) and MODIS dataset. Experimental results have confirmed that the accuracy of implemented classified maps significantly increases with the fusion of both datasets as compared to the individual implementation of SCATSAT-1- and MODIS-classified maps. From quantitative analysis, the RF classifier performs better as compared to other classifiers, i.e. ANN, SAM, and SVM on the fused dataset. This study has many applications in the near real-time monitoring of snow/ice, agriculture activities, and hydrological studies.

41. GIMD-Net: An effective General-purpose Image Manipulation Detection Network, even under anti-forensic attacks
G Singh, P Goyal – IEEE International Joint Conference on Neural Networks, 2021

Abstract: The digital image information can be easily tampered to harm the integrity of someone. Thus, recognizing the truthfulness and processing history of an image is one of the essential concerns in multimedia forensics. Numerous forensic methods have been developed by researchers with the ability to detect targeted editing operations. But, creating a unified forensic approach capable of detecting multiple image manipulations is still a challenging problem. In this paper, a new GIMD network is designed that exploits local dense connections and global residual learning for better classification by using robust residual dense blocks (RDBs). The network input and high-level hierarchical features produced by proposed residual dense blocks are fused globally for better information flow across the network. The extensive experiment results show that the proposed scheme outperforms the existing state-of-the-art general-purpose forensic schemes even under anti-forensic attacks, when tested on large scale publicly available datasets. Our model offers overall detection accuracies of 95.09% and 97.31 % for BOSSBase and Dresden datasets, respectively for multiple image manipulation detection.

42. Highly efficient metal/solvent-free chemical fixation of CO_2 at atmospheric pressure conditions using functionalized porous covalent organic frameworks
G Singh, CM Nagaraja - Journal of CO2 Utilization, 2021

Abstract: The development of metal-free heterogeneous catalysts for selective carbon capture and utilization (CCU) as a C1-feedstock under mild conditions has significant potential towards sustainable fixation of atmospheric CO_2 into value-added products. Herein, we report utilization of polar functionalized covalent-organic framework (COF-SO_3H) as metal-free heterogeneous catalyst for efficient fixation of CO_2 into cyclic carbonates. The COF-SO_3H possesses large 1D channels functionalized with polar (–NH, and –SO3H) groups rendering selective adsorption property for CO_2 with a high heat of interaction (Qst) energy of 42.2 kJ/mol. Interestingly, the value of Qst for COF-SO_3H was found to be about 10.8 kJ/mol higher than that of analogous COF (COF-H) which lacks the polar sulfonic acid group. The presence of basic –NH sites combined with Brønsted acid (–SO_3H) sites make COF-SO_3H a suitable material for metal/solvent-free chemical fixation of CO_2 with epoxides. Indeed, COF-SO_3H catalyzes cycloaddition of CO_2 with epoxides to generate cyclic carbonates under metal/solvent-free atmospheric pressure conditions. Moreover, COF-SO_3H is highly recyclable for several cycles with retaining the catalytic activity and structural rigidity. This work represents a rare demonstration of metal/solvent-free chemical fixation of CO_2 under atmospheric pressure conditions using polar-functionalized COF.

Graphical Abstract:
A rare demonstration of metal/solvent-free chemical fixation of CO_2 into value-added cyclic carbonates under mild atmospheric pressure conditions using polar-functionalized COF is presented.

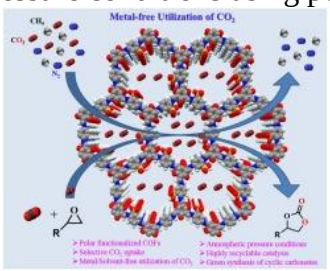

43. [Immunotherapeutic Role of NOD-2 and TLR-4 Signaling as an Adjunct to Antituberculosis Chemotherapy]
M Aqdas, SK Maurya, S Pahari, S Singh, N Khan… G Kaur, JN Agrewala - ACS Infectious Diseases, 2021

Abstract: Tuberculosis (TB) treatment is lengthy and inflicted with severe side-effects. Here, we attempted a novel strategy to reinforce host immunity through NOD-like receptor (NOD-2) and Toll-like receptor (TLR-4) signaling in the murine model of TB. Intriguingly, we noticed that it not only bolstered the immunity but also reduced the dose and duration of rifampicin and isoniazid therapy. Further, we observed expansion in the pool of effector ($CD44^{hi}$, $CD62L^{lo}$, $CD127^{hi}$) and central ($CD44^{hi}$, $CD62L^{hi}$, $CD127^{hi}$) memory CD4 T cells and CD8 T cells and increased the intracellular killing of Mycobacterium tuberculosis (Mtb) by activated dendritic cells [$CD86^{hi}$, $CD40^{hi}$, IL-6^{hi}, IL-12^{hi}, TNF-α^{hi}, nitric oxide $(NO)^{hi}$] with significant reduction in Mtb load in the lungs and spleen of infected animals. We infer that the signaling through NOD-2 and TLR-4 may be an important approach to reduce the dose and duration of the drugs to treat TB.

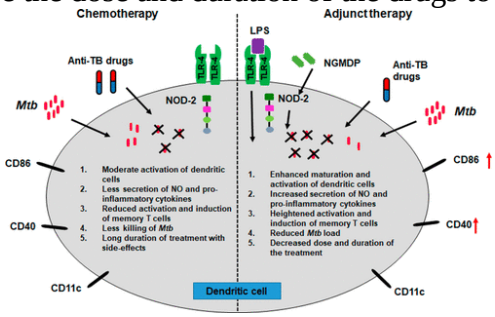

44. [Impact of Natural Disasters on Energy Consumption: Evidence From Indian States]
B Rakshit – Energy Research Letters, 2021

Abstract: This study investigates the impact of natural disasters on energy consumption across selected Indian states from 1996 to 2019. Using the system generalized method of moments, we examine whether the frequent occurrence of floods and droughts alters India's energy demand. Our findings show considerable variation in the relation between natural disasters and energy consumption. Generally, we find that natural disasters, as measured by the magnitude of floods and a drought dummy, have an adverse impact on per capita energy consumption.

45. [Implementation of managed aquifer recharge techniques in India]
S Ganguly, S Ganguly – Current Science, 2021

Abstract: Rapid rise in population and urbanization have caused excessive groundwater exploitation which is a major concern. Therefore, technologies to replenish the groundwater are necessary for its conservation and sustainable development. Storage of freshwater in shallow aquifers using different techniques has become the practice worldwide to restore the depleting groundwater and improve water quality. This article addresses the implementation of managed aquifer recharge (MAR) in six zones of India, viz. North, South, East, West, Central and North East along with a brief scenario of the geologies of these zones. The prevalence of percolation tanks, check dams, recharge shafts and rainwater harvesting methods is found to be feasible and beneficial in most parts of India due to their efficiency and easy application. The adversities of MAR like clogging of porous media are also highlighted along with their mitigation strategies.

46.	Investigating neutron transfer in the ^{9}Be + ^{197}Au system M Kaushik, SK Pandit, VV Parkar, S Thakur…RG Pillay, PP Singh – Physical Review C, 2021 **Abstract**: In this work n-transfer and incomplete fusion cross sections for the ^{9}Be + ^{197}Au system are reported over a wide energy range, $E_{c.m.}$≈29−45 MeV. The experiment was carried out using the activation technique and off-line γ counting. The transfer process is found to be the dominant mode as compared to all other reaction channels. Detailed coupled reaction channel (CRC) calculations have been performed for n-transfer stripping and pickup cross sections. The measured 1n-stripping cross sections are explained with CRC calculations by including the ground state and the 2^{+} resonance state (E=3.03 MeV) of ^{8}Be. The calculations for 1n-pickup cross sections, including only the ground state of 10Be agrees reasonably well with the measured cross sections, while it overpredicts the data at subbarrier energies. For better insight into the role of the projectile structure in the transfer process, a comprehensive analysis of the 1n-stripping reaction has been carried out for various weakly bound projectiles on a ^{197}Au target nucleus. The transfer cross sections scaled with the square of the total radius of interacting nuclei show the expected Q-value dependence of the 1n-stripping channel for weakly bound stable projectiles.
47.	Investigation of charge transport and band alignment of MoS2-ReS2 heterointerface for high performance and self-driven broadband photodetection R Wadhwa, AV Agrawal, D Kushavah, A Mushtaq, SK Pal, M Kumar - Applied Surface Science, 2021 **Abstract**: Two dimensional (2D) van der Waals heterostructures are becoming one of the ascendant research areas for semiconducting device application owing to their remarkable optoelectronic properties, which allows more functioning ability beyond its individual constituent. 2D layered materials can be easily integrated and form heterostructure due to the dangling bond free surfaces. However, for novel optoelectronic device applications, the understanding of charge carrier dynamics at the interface of heterostructures is critical and essential. Here, we demonstrate the charge transport behaviour and energy level band alignment at MoS2-ReS2 heterointerface. Interlayer coupling and charge transport behaviour are investigated by Raman and photoluminescence spectroscopy. The photoelectron spectroscopy confirms type II band alignment between MoS2-ReS2 interface, which is required for efficient separation and transportation of charge carriers. As a proof of concept, a highly sensitive, self-biased broadband photodetector is fabricated with a responsivity of 42.61 A/W at a low bias of 1 V under the illumination of 800 nm, which is 16 fold higher than the reference pristine MoS2 photodetector. Moreover, fast rise/decay transient photoresponse (20/19 ms) strongly advocate the spatial separation of charge carriers across the interface. Our proposed work establishes the MoS2 and ReS2 as promising candidates for next-generation broadband photodetector applications. **Graphical Abstract**: 2D heterostructures have paved the way for the next generation optoelectronics. Investigation of band-alignment and carrier dynamic is beneficial to design the heterostructures for photodetector applications. Here, band-alignment and charge transport is studied at MoS2-ReS2 heterointerface for high performance broadband photodetector. Heterojunction shows self-driven feature with enhanced photoresponse than pristine MoS2, attributed to the favourable type II alignment at the heterointerface.

	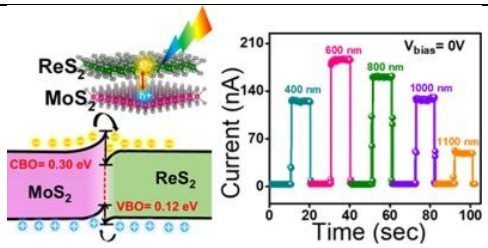
48.	Is Wikipedia Easy to Understand?: A Study Beyond Conventional Readability Metrics S Setia, SRS Iyengar, AA Verma, N Dubey - International Conference on Computational Collective Intelligence: Part of the Communications in Computer and Information Science book series, 2021 **Abstract**: Wikipedia has emerged to be one of the most prominent sources of information available on the Internet today. It provides a collaborative platform for editors to edit and share their information, making Wikipedia a valuable source of information. The Wikipedia articles have been duly studied from an editor's point of view. But, the analysis of Wikipedia from the reader's perspective is yet to be studied. Since Wikipedia serves as an encyclopedia of information for its users, its role as an information securing tool must be examined. The readability of a written text plays a major role in imparting the intended comprehension to its readers. Readability is the ease with which a reader can understand the underlying piece of text. In this paper, we study the readability of various Wikipedia articles. Apart from judging the readability of Wikipedia articles against standard readability metrics, we introduce some new parameters related specifically to the comprehension of the text present in Wikipedia articles. These new parameters, combined with standard readability metrics, help classify the Wikipedia articles into comprehensible and non-comprehensible classes through the SVM classification technique.
49.	K-Preferential Slotted ALOHA for Ultra Reliable Low Latency Communications S Agarwal, S Pandey – IEEE National Conference on Communications, 2021 **Abstract**: Ultra-reliable low-latency communication (URLLC), one of the key component of 5G, provides a set of features required to support mission-critical applications. Slotted ALOHA is one of the most popular mechanism to share a channel among multiple users. However, slotted ALOHA cannot meet high reliability requirements of URLLC when large number of users are present in the network. In this paper, we propose a preferential medium access control scheme to match the high reliability requirement of URLLC. It is ensured by dedicating every Kth slot exclusively for URLLC transmission. We analytically obtain the packet delay distribution and reliability of both the URLLC and regular packets. An optimization problem is framed to maximize the reliability of regular packets subject to meeting the URLLC reliability constraints. Extensive simulations indicate that our proposed K -preferential S-ALOHA protocol can meet the URLLC requirements even when the network traffic is high.
50.	Laparoscopic Lens Defogging: a Review of Methods to Maintain a Clear Operating Field R Kumar, S Jallu, K Pasricha, B Basumatary, BPS Parmar, AK Sahani - Indian Journal of Surgery, 2021 **Abstract**: One of the fundamental principles of a successful laparoscopic procedure is a clear operating field. The laparoscopic lens must be able to visualize the internal organs as clearly as possible. However, fogging on the laparoscopic lens due to temperature gradient poses an obstruction in the field of view for surgeons. Many techniques like insufflation, irrigation system, antifogging solutions, and heat source have been employed in order to avoid the fogging of these lenses, but all these methods are partially effective, require constant supervision, and are time-

	consuming. Therefore, antifogging ability combined with high transparency is imperative for the fabrication of such lenses. In this review, different methods of defogging of laparoscopic lenses are discussed. However, in order to overcome the shortcomings of these methods, another method of defogging laparoscopic lens using superhydrophobic coatings is presented in this review. It discusses different types of organic, inorganic, and hybrid materials for fabrication of superhydrophobic glass substrates. These materials include silica-based nanoparticles, metallic oxides, and polymers. While silica-based particles have shown immense promise as potential candidates for transparent superhydrophobic materials because of development of high contact angles, polymers are also being widely employed for this purpose due to various advantages that they present.
51.	MAIRE - A Model-Agnostic Interpretable Rule Extraction Procedure for Explaining Classifiers R Sharma, N Reddy, V Kamakshi, NC Krishnan, S Jain - International Cross-Domain Conference for Machine Learning and Knowledge Extraction: Part of the Lecture Notes in Computer Science book series, 2021 **Abstract**: The paper introduces a novel framework for extracting model-agnostic human interpretable rules to explain a classifier's output. The human interpretable rule is defined as an axis-aligned hyper-cuboid containing the instance for which the classification decision has to be explained. The proposed procedure finds the largest (high coverage) axis-aligned hyper-cuboid such that a high percentage of the instances in the hyper-cuboid have the same class label as the instance being explained (high precision). Novel approximations to the coverage and precision measures in terms of the parameters of the hyper-cuboid are defined. They are maximized using gradient-based optimizers. The quality of the approximations is rigorously analyzed theoretically and experimentally. Heuristics for simplifying the generated explanations for achieving better interpretability and a greedy selection algorithm that combines the local explanations for creating global explanations for the model covering a large part of the instance space are also proposed. The framework is model agnostic, can be applied to any arbitrary classifier, and all types of attributes (including continuous, ordered, and unordered discrete). The wide-scale applicability of the framework is validated on a variety of synthetic and real-world datasets from different domains (tabular, text, and image).
52.	MSAR-Net: Multi-scale attention based light-weight image super-resolution N Mehta, S Murala - Pattern Recognition Letters, 2021 **Abstract**: Recently, single image super-resolution (SISR), aiming to preserve the lost structural and textural information from the input low resolution image, has witnessed huge demand from the videos and graphics industries. The exceptional success of convolution neural networks (CNNs), has absolutely revolutionized the field of SISR. However, for most of the CNN-based SISR methods, excessive memory consumption in terms of parameters and flops, hinders their application in low-computing power devices. Moreover, different state-of-the-art SR methods collect different features, by treating all the pixels contributing equally to the performance of the network. In this paper, we take into consideration both the performance and the reconstruction efficiency, and propose a Light-weight multi-scale attention residual network (MSAR-Net) for SISR. The proposed MSAR-Net consists of stack of multi-scale attention residual (MSAR) blocks for feature refinement, and an up and down-sampling projection (UDP) block for edge refinement of the extracted multi-scale features. These blocks are capable of effectively exploiting the multi-scale edge information, without increasing the number of parameters. Specially, we design our network in progressive fashion, for substituting the large scale factors (x 4) combinations, with small scale factor (x 2) combinations, and thus gradually exploit the hierarchical information. In parallel, for modulation of multi-scale features in global and local manners, channel and spatial attention in MSAR block is

	being used. Visual results and quantitative metrics of PSNR and SSIM exhibit the accuracy of the proposed approach on synthetic benchmark super-resolution datasets. The experimental analysis shows that the proposed approach outperforms the other existing methods for SISR in terms of memory footprint, inference time and visual quality.
53.	Multi-frame based Adversarial Learning Approach for Video Surveillance PW Patil, A Dudhane, S Chaudhary, S Murala - Pattern Recognition, 2021 **Abstract**: Foreground-background segmentation (FBS) is one of the prime tasks for automated video-based applications like traffic analysis and surveillance. The different practical scenarios like weather degraded videos, irregular moving objects, dynamic background, etc., make FBS a challenging task. The existing FBS algorithms mainly depend on one of the three different factors, namely (1) complicated training process, (2) additionally trained modules for other applications, or (3) neglect the inter-frame spatio-temporal structural dependencies. In this paper, a novel multi-frame-based adversarial learning network is proposed with multi-scale inception and residual module for FBS. As, FBS is a temporal enlightenment-based problem, a temporal encoding mechanism with decreasing variable intervals is proposed for the input frame selection. The proposed network comprises multi-scale inception and residual connection-based dense modules to learn prominent features of the foreground object(s). Also, feedback of the estimated foreground map of previous frame is utilized to exhibit more temporal consistency. Learning of the network is concentrated in different ways like cross-data, disjoint, and global training-testing for FBS. The qualitative and quantitative experimental analysis of the proposed approach is done on three benchmark datasets for FBS. Experimental analysis on three benchmark datasets proves the significance of the proposed approach as compared to state-of-the-art FBS approaches.
54.	New experimental approach for developing a mass-energy systematics for precompound emission MK Sharma, M Sarswat, S Arora, S Kumar, M Shuaib…PP Singh… - Physical Review C, 2021 **Abstract**: A systematic analysis of the experimental cross-section data in odd mass number (A) and odd atomic number (Z) nuclei is reported to reveal a novel mass-energy systematics for the pre-compound emission of fast neutrons in α-induced reactions at low energies. The experimental excitation functions have been analyzed within the framework of statistical model predictions to get information regarding pre-compound emission. The present analysis establishes for first time an interesting systematics, emphasizing that accessible excitation energy on peripheral nucleons of the systems is an exponential function of atomic mass number (A) of target nuclei. One of the most important features of this systematics is to provide a precise estimation of the pre-compound contribution for any nuclei, except closed-shell ones, over a wide range of mass number $63 \leq A \leq 109$ in the nuclear landscape. New results of the present analysis emphasize an additional subtle interconnection between the structure of nuclei and the nuclear reaction mechanism of the pre-compound emission process at low energies, where the compound nucleus process is more likely to be dominant.
55.	On the Effect of Noise Induced Dynamics on Linear Growth Rates of Oscillations in an Electroacoustic Rijke Tube Simulator N Vishnoi, P Wahi, A Saurabh, L Kabiraj - ASME Turbo Expo 2021: Turbomachinery Technical Conference and Exposition, 2021 **Abstract**: Suppressing self-excited thermoacoustic oscillations in combustion chambers is essential for gas turbine system stability. Passive acoustic damping devices such as Helmholtz resonators are commonly employed in modern combustors to address the problem of thermoacoustic instabilities. The estimation of deterministic parameters characterizing flame-acoustic coupling, specifically the stability margins and linear growth/decay rates, is a prerequisite for designing these devices. As gas turbine combustors are typically noisy systems due to the presence of highly turbulent flows and

	unsteady combustion, it is essential to understand the role of noise and its impact on the estimated system stability. Recently several new results on the stochastic dynamics of thermoacoustic systems and the use of noise-induced dynamics to estimate system stability characteristics have been reported. In the present work, we study the different approaches previously reported on the estimation of linear growth/decay rates from noise-induced dynamics on an electroacoustic Rijke tube (a prototypical thermoacoustic system) simulator. We estimate the growth rates from noisy data obtained from the subthreshold, bistable, and linearly-unstable regions of the observed subcritical Hopf bifurcation and investigate the effect of additive noise intensity. We find that the noise intensity affects the stability boundaries and the estimated growth rates.
56.	Optomechanical isolation with tunable center frequency C Waghela, S Dasgupta - Journal of Physics B: Atomic, Molecular and Optical Physics, 2021 **Abstract**: Optomechanical isolators have the ability to stop the optical field for one direction and to pass the field in the opposite direction. Thus they work as bandstop filter in one direction and bandpass filter in the opposite direction. The maximum isolation happens when the frequency of the field becomes equal to that of the mechanical membrane inside the isolator. This frequency, called the isolation (or center) frequency, however is restricted by the fact that the fundamental frequency of the membrane depends upon its physical parameters (such as mass and length), which are fixed during fabrication of the membrane. We propose a dynamical way of tuning this center frequency, by using a mechanical drive attached to a membrane with quadratic optomechanical coupling in a membrane-in-the-middle setup. This provides a way for future applications where tunable filtering is required.
57.	Pattern-Based Colorimetric Sensor Array to Monitor Food Spoilage using Automated High-Throughput Analysis H Singh, G Singh, N Kaur, N Singh - Biosensors and Bioelectronics, 2021 **Abstract**: Despite the existing rapid and reliable analytical methods for determining biogenic amine in food matrices, recently special efforts have been devoted for development of portable and inexpensive devices for discrimination of biogenic amines (BAs) in food products to achieve onsite detection of food-spoilage. Thus, in this context, a field deployable cross-reactive sensor array and a field-portable array reader has been developed for determination of food quality. The sensor array consisting of metal complexes (C1 – C11) of single azophenol dye-based receptor generated a unique visible response on interaction with different amines (A1 – A7). Further, the colorimetric pattern and discrimination efficacy of the sensor array was evaluated using multivariate statistical techniques such as principal component analysis and linear discriminant analysis. Motivated by outstanding discriminatory power of sensor array, titration experiment was performed with BAs, and colorimetric response of array was linearly corelated to concentrations of BAs such as tryptamine and spermine with R2 values of 0.9596 and 0.967 respectively. Finally, for practical utility and the field analysis, a portable reader was developed and utilized for quantification of biogenic amines in meat and cottage cheese samples spiked with spermine and tryptamine up to the concentrations of 40 μM; therefore, apparently proving the potential applicability of the designed sensing method for food quality monitoring.
58.	Phase stability, mechanical, thermal, electronic properties, anisotropy, lattice dynamics and APB-energies of Ti2AlX intermetallics in α2, B2, and O phases: A First principle study K Goyal, C Bera, N Sardana - Materials Today Communications, 2021 **Abstract**: The ternary titanium aluminide based alloys have been lucrative for high-temperature applications in next-generation aerospace vehicles. Present work systematically investigates phase stability, structural and elastic properties of Ti2AlX (Xdouble bondMo, W, Ta, Nb, Zr, Hf) in α2,

	B2 and, O phases, calculated using density functional theory (DFT) within generalized gradient approximation (GGA). The Pugh's ratio, Poisson's ratio, Cauchy pressures, Vicker's hardness, machinability index, anisotropies, Debye temperature, thermal conductivity, melting temperature, and Peierls stress, derived from the elastic constants are also presented. Phonon calculations reveal that Ti_2AlX (Xdouble bondMo, W) in their α2 phase are dynamically unstable. The dominant slip systems are predicted from antiphase boundary (APB) energy calculations which indicate that dominance and mobility of the slip systems are largely affected by the ternary element 'X′ and explains its ductile-brittle behavior. The bonding behavior is also investigated using the electronic density of states plots. The increased Ti-X bonding enhances while increased Ti-Al bonding degrades the ductility in Ti_2AlX intermetallics. **Graphical Abstract**: 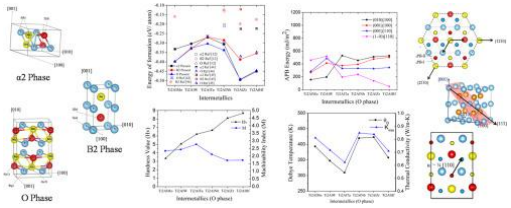
59.	Prediction of Cyclic Plastic Strain Energy Density and Fatigue Life of Non-Masing Behavior Materials Without Master Curve SS Yadav, SC Roy, J Veerababu, S Goyal - Transactions of the Indian National Academy of Engineering, 2021 **Abstract**: Masing/non-Masing behavior of material plays an important role in the strain energy-based methods of fatigue life prediction. Materials under fatigue are found to show three distinct categories of behavior viz. Masing, non-Masing (Type-I: when master curve can be constructed) and non-Masing (Type-II: when master curve cannot be constructed). The master curve method available in the literature for the estimation of cyclic plastic strain energy density (CPSED) can be used only for Type-I non-Masing and Masing behaviors of materials. Moreover, it could be used for estimation only, not for prediction of CPSED. Very recently (in 2021), a new method, as summarized in this article, was proposed for the prediction of CPSED and fatigue life of material irrespective of Masing or non-Masing (Type-I and Type-II) behavior. Although the method was developed, the validation of the proposed method with different Type-II non-Masing behavior materials remained a matter of further investigation. As Type-II non-Masing behavior was not highlighted earlier in the literature, such data is not readily available. In this article, we conducted low cycle fatigue tests on SS 304L material, and after an extensive literature review and analysis, three materials' data for each of Type-I and Type-II non-Masing behaviors could be collected. The method of prediction of CPSED and fatigue life is summarized and implemented on the six different materials. The CPSED and fatigue life could be predicted within a scatter band of 1.2 and 2, respectively. This article confirms the universal nature of the new method of CPSED and fatigue life prediction.
60.	Quantifying the Impact of Biopics on Wikipedia Articles AA Verma, N Dubey, S Setia, P Kamtam, SRS Iyengar - Journal of Cases on Information Technology, 2022 **Abstract**: Wikipedia is known for its extensive and comprehensive knowledge of multifarious topics. These topics are maintained as articles along with a history of versions of these articles, these versions are also known as revisions. Revisions are the results of edits made by various users. Here, the authors analyze biographical Wikipedia articles, mainly biographies that have a movie based on

	them re- leased after the year 2010. The authors look at the impact of the movie release on its corresponding biography article on Wikipedia by looking at various metrics of each revision in a Wikipedia article and analyze how the revisions closer to the movie's release date compare with the rest of the revisions. The results show that quality and content in Wikipedia articles increases significantly during the release time frame of corresponding biopics. The authors believe their work will stimulate more research in the direction of understanding Wikipedia's relationship with its allied portals.
61.	Selective Production of Secondary Amine By the Photocatalytic Cascade Reaction Between Nitrobenzene and Benzyl alcohol over Nanostructured Bi2MoO6 and Pd NPs Decorated Bi2MoO6 R Srivastava, R Ghalta, AK Kar – Chemistry - An Asian Journal, 2021 **Abstract**: The synthesis of secondary amine by the photo alkylation of nitrobenzene with benzyl alcohol using a simple light source and Sunlight is challenging. Herein one-pot cascade protocol is employed to synthesize secondary amine by the reaction of nitrobenzene and benzyl alcohol. The one-pot cascade protocol involves four reactions: (a) photocatalytic reduction of nitrobenzene to aniline, (b) photocatalytic oxidation of benzyl alcohol to benzaldehyde, (c) reaction between aniline and benzaldehyde to form imine, and (d) photocatalytic reduction of imine to a secondary amine. The cascade protocol to synthesize secondary amine is accomplished using Bi 2 MoO 6 , and Pd nanoparticles decorated Bi 2 MoO 6 catalysts. The surface characteristics, oxidation states, and elemental compositions of the materials are characterized by several physicochemical characterization techniques. Optoelectronic and photoelectrochemical measurements are carried out to determine the bandgap, band edge potentials, photocurrents, charge carrier's separation, etc. An excellent yield of secondary amine is achieved with simple household white LED bulbs. The catalyst also exhibits similar or even better activity in Sunlight. The structure-activity relationship is established using catalytic activity data, control reactions, physicochemical, optoelectronic characteristics, and scavenging studies. Bi 2 MoO 6 and Pd nanoparticles decorated Bi 2 MoO 6 exhibit excellent photostability and recyclability. The simple catalyst design with sustainable and economical light source for the synthesis of very useful secondary amine from the nitrobenzene and benzyl alcohol would attract the researchers to develop similar catalytic protocols for other industrially important chemicals.
62.	Simplified Macro Modeling Approach for Estimation of Nonlinear Response of Infilled RC Frames PL Kurmi, P Haldar - Recent Advances in Earthquake Engineering: Part of the Lecture Notes in Civil Engineering book series, 2021 **Abstract**: The manuscript proposes a simplified macro modeling approach to estimate the in-plane nonlinear response of infilled RC frames efficiently. The most commonly used macro modeling technique for the simulation of infill in RC frame is using an equivalent diagonal pin-jointed compressive strut. The present modeling approach extends the same technique and predicts the initial stiffness, peak strength, and overall load-deformation behavior with a more accurate approximation as compared to ASCE 41-06 model. The proposed model modifies the elastic modulus of the equivalent strut and RC column system based on the initial stiffness of the infilled RC frame. The accuracy of the proposed procedure is evaluated with the backbone envelopes of 12 single-bay, single-storey physically tested infilled RC frames. Comparison of numerically developed capacity curves with the experimental envelopes shows that the peak strength predicted by the proposed model is in good agreement with experimental data. Also, a good approximation of the initial stiffness of the infilled frame has been achieved. The proposed simplified macro modeling approach is an improvement over the widely used ASCE 41-06 infill model in estimating the initial stiffness, peak strength, and overall load-deformation behavior.

63.	Singularity analysis of a 7-DOF spatial hybrid manipulator for medical surgery S Gupta, E Singla, S Soni, A Singla - International Journal of Nonlinear Sciences and Numerical Simulation, 2021 **Abstract**: This paper presents the singularity analysis of a 7-degrees of freedom (DOF) hybrid manipulator consisting of a closed-loop within it. From the past studies, it is well-known that the kinematic singularities play a significant role in the design and control of robotic manipulators. Kinematic singularities pose two-fold effects – first, they can induce the loss of one or more DOF of the manipulator and cause infinite joint rates at that particular joint, and second, they help to determine the trajectory or zone with high mechanical advantage. In current work, a 7-DOF hybrid manipulator is considered which is being developed at Council Of Scientific And Industrial Research–Central Scientific Instruments Organisation (CSIR–CSIO) Chandigarh to assist a surgeon during a medical-surgical task. To emulate the natural motion of a surgeon, the challenging configuration with redundant DOF is utilized. Jacobian has been computed analytically and analyzed at each instantaneous configuration with the evaluation of manipulability. Effect of a closed loop in the hybrid configurations is focused at, and utilizing the contour plots, good and worst working zones are identified in the workspace of the manipulator. The verification and validation of best and worst manipulability points (singularities) are done with the help of genetic algorithms, to determine locally and globally optimal configurations. Finally, on the basis of the singularity analysis, the present work concludes with few guidelines to the surgeon about the best and worst working zones for surgical tasks.
64.	Solar air heater having multiple V-ribs with Multiple-Symmetric gaps as roughness elements on Absorber-Plate: A parametric study AS Kashyap, R Kumar, P Singh, V Goel - Sustainable Energy Technologies and Assessments, 2021 **Abstract**: Conversion of solar energy into thermal energy using solar collectors is the most promising way for its applicability. Artificial roughness applied underside of the solar heat-collector is a preferably advantageous technique to enhance the solar air heater performance. In the present study, a comprehensive parametric analysis of the multi-V-ribs-with-symmetric-multi-gaps type of roughness elements (which employed over the heat-collector plate) has been conducted. Two novel roughness parameters (discreteness ratio and aspect ratio) are introduced and their impact is analyzed on thermo-hydraulic performance of the solar air heater (SAH). Moreover, relative roughness width, relative gap width, relative rib-height and relative rib-pitch impact are also assessed. The output parameter (i.e., Nusselt number and friction factor) has been estimated from the experimentally measured data under steady-state conditions. An increment of 6.46 times in Nusselt number along with 5.67 times in friction factor is observed in a comparison to a smooth SAH. The maximum thermo-hydraulic performance parameter for the present investigation is 4.24, which is comparatively higher. The generalized mathematical expressions for Nusselt number and friction factor are developed. The predicted results are found in the deviation of 7.28% and 8.45% for Nusselt number and friction factor.
65.	Techniques to Improve Write and Retention Reliability of STT-MRAM Memory Subsystem S Sethuraman, VK Tavva, MB Srinivas - IEEE Transactions on Computer-Aided Design of Integrated Circuits and Systems, 2021 **Abstract**: Spin transfer torque magneto-resistive random-access memory (STT-MRAM) has many advantages, such as scalability, persistence, practically infinite endurance, and fast access speed, that make it a promising and emerging technology for memory. However, this technology has multiple reliability issues such as read and write reliability, higher write power, and long write latency, etc. At elevated temperatures, these issues exacerbate further. As the temperature increases massively in

	the latest compute nodes, we need to study and understand the effect of temperature on STT-MRAM memory writes and reliability. In this paper, we propose temperature-aware memory controller and device architecture techniques specific to STT-MRAM technology, that can improve write reliability, retention reliability, and memory power without sacrificing the performance. Our simulation results show that the proposed techniques cumulatively improve write BER on an average by 603X, increase retention reliability by 65%, along with 27% power reduction and 5.8% improved system performance over the baseline STT-MRAM based memory subsystem.
66.	Temperature-Controlled Chemoselective Synthesis of Thiosulfonates and Thiocyanates: Novel Reactivity of KXCN (X= S, Se) Towards Organosulfonyl Chlorides P Kalaramna, A Goswami - European Journal of Organic Chemistry, 2021 **Abstract**: An efficient chemoselective protocol has been developed for the synthesis of thiosulfonates and thiocyanates by employing cost effective and commercially available organosulfonyl chlorides with potassium thio-/selenocyanate. The strategy offered the thiosulfonates and thiocyanates selectively by tuning the equivalents of KSeCN and optimizing the reaction temperature. On the other hand, thiosulfonates were obtained as sole products when organosulfonyl chlorides treated with KSCN. Furthermore, synthesis of diarylthioethers and aryl(heteroaryl) thioethers were carried out as a part of synthetic application of newly prepared arylthiocyanates.
67.	The Gordian complex of theta-curves S Joshi, M Prabhakar - Journal of Knot Theory and Its Ramifications, 2021 **Abstract**: In this paper, we study the Gordian metric on the set of all theta-curves and give a lower bound of it. We define the Gordian complex of theta-curves, which is a simplicial complex whose vertices consist of all theta-curves in the 3-dimensional Euclidean space R^3. We show that for any given theta-curve Θ, there exists an infinite family of theta-curves containing Θ such that the Gordian distance between any two distinct members of this family is equal to one.
68.	This Explains That: Congruent Image–Report Generation for Explainable Medical Image Analysis with Cyclic Generative Adversarial Networks A Pandey, B Paliwal, A Dhall, R Subramanian… - International Workshop on Interpretability of Machine Intelligence in Medical Image Computing: Part of the Lecture Notes in Computer Science book series, 2021 **Abstract**: We present a novel framework for explainable labeling and interpretation of medical images. Medical images require specialized professionals for interpretation, and are explained (typically) via elaborate textual reports. Different from prior methods that focus on medical report generation from images or vice-versa, we novelly generate congruent image–report pairs employing a cyclic-Generative Adversarial Network (cycleGAN); thereby, the generated report will adequately explain a medical image, while a report-generated image that effectively characterizes the text visually should (sufficiently) resemble the original. The aim of the work is to generate trustworthy and faithful explanations for the outputs of a model diagnosing chest X-ray images by pointing a human user to similar cases in support of a diagnostic decision. Apart from enabling transparent medical image labeling and interpretation, we achieve report and image-based labeling comparable to prior methods, including state-of-the-art performance in some cases as evidenced by experiments on the Indiana Chest X-ray dataset.
69.	Tribological Behavior of Cold-Sprayed Titanium/Baghdadite Composite Coatings in Dry and Simulated Body Fluid Environments A Kumar, R Kant, H Singh - Surface and Coatings Technology, 2021 **Abstract**: This study reports the tribological behavior of Titanium/Baghdadite cold sprayed

	composite coatings for artificial human joints in a dry and simulated body fluid environments. Sliding wear tests are performed using a wear test rig to predict the wear resistance of the coatings. An in-depth analysis of the worn-out coatings is also done to establish the wear mechanism for the developed coatings. Scratch adhesion and wettability analyses of the composite coatings have also been reported. The role of microhardness and surface roughness on the performance of the cold sprayed composite coatings is also discussed. It is discovered that cold sprayed composite coatings successfully protect the biomedical grade steel from wear in dry and simulated body fluid environments. Three-body abrasion wear and adhesive wear are the dominant mechanisms observed behind the wear of these coatings. Coatings are found to adhere well with the substrate, and the critical loads for the coatings' delamination are also reported. Furthermore, the coatings are found to be hydrophilic in nature, and the hydrophilicity is observed to be improving with an increase in baghdadite content.
70.	Ultrathin Lubricant-Infused Vertical Graphene Nanoscaffolds for High-Performance Dropwise Condensation A Tripathy, CWE Lam, D Davila…CS Sharma… - ACS Nano, 2021 **Abstract**: Lubricant-infused surfaces (LIS) are highly efficient in repelling water and constitute a very promising family of materials for condensation processes occurring in a broad range of energy applications. However, the performance of LIS in such processes is limited by the inherent thermal resistance imposed by the thickness of the lubricant and supporting surface structure, as well as by the gradual depletion of the lubricant over time. Here, we present an ultrathin (∼70 nm) and conductive LIS architecture, obtained by infusing lubricant into a vertically grown graphene nanoscaffold on copper. The ultrathin nature of the scaffold, combined with the high in-plane thermal conductivity of graphene, drastically minimize earlier limitations, effectively doubling the heat transfer performance compared to a state-of-the-art CuO LIS surface. We show that the effect of the thermal resistance to the heat transfer performance of a LIS surface, although often overlooked, can be so detrimental that a simple nanostructured CuO surface can outperform a CuO LIS surface, despite filmwise condensation on the former. The present vertical graphene LIS is also found to be resistant to lubricant depletion, maintaining stable dropwise condensation for at least 24 h with no significant change of advancing contact angle and contact angle hysteresis. The lubricant consumed by the vertical graphene LIS is 52.6% less than that of the existing state-of-the-art CuO LIS, also making the fabrication process more economical. 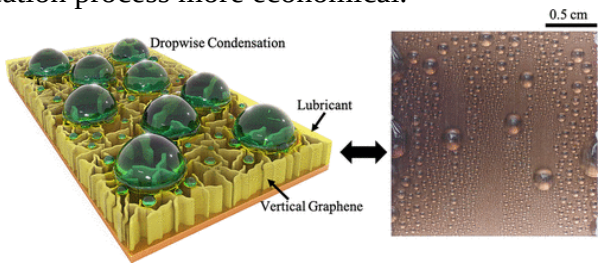
71.	Understanding the effect of processing temperature and carbon nanotube addition on the viscoelastic response of polyurethane foams J Bhinder, PK Agnihotri - Journal of Applied Polymer Science, 2021 **Abstract**: We experimentally demonstrate a strategy to design the microstructure and hence viscoelastic behavior of polyurethane (PU) foams. PU foams are fabricated at two temperatures (room and −5°C) and reinforced with varying concentrations of oxidized carbon nanotubes (CNTs). Hierarchical pores, thicker cell walls, higher density, and low porosity are recorded in PU foams processed at −5°C. The addition of CNTs improves the cell wall stiffness and thermal stability of

	PU foams. Master curves constructed from dynamic mechanical analysis show that processing at −5°C and addition of 1.6 wt.% oxidized CNTs enhance the storage modulus of PU foams over a wide temperature and frequency range. Prony series analysis reveals that PU foams fabricated at −5°C have significantly lower relaxation time. Moreover, the elastic modulus of PU foams processed using optimized conditions shows stronger rate dependency in comparison to other types of PU foams fabricated in this work.
72.	Utilisation of spaceborne C-band dual pol Sentinel-1 SAR data for simplified regression-based soil organic carbon estimation in Rupnagar, Punjab, India A Tripathi, RK Tiwari - Advances in Space Research, 2021 **Abstract**: Soil Organic Carbon (SOC) is a measure of the total carbon content of the soil and is a vital soil health indicator. Over the decades, SOC has been estimated using sampling followed by rigorous laboratory-based testing methods. Spaceborne Microwave/Synthetic Aperture RADAR (SAR) remote sensing has proven to be a versatile tool for various soil study applications. However, there have been very few studies conducted for SOC estimation using SAR remote sensing. This study utilises time-series, C-band remotely sensed SAR data from Sentinel-1 A satellite for SOC estimation and compared the performances of Random Forest (RF) and Ordinary Least Squares (OLS) Regression models over agricultural areas of Rupnagar district of Punjab in India. A set of 96 soil samples were collected from 32 different agricultural field locations in Rupnagar district between November 2019 to January 2020. SAR backscatter of Vertically emitted and Vertically received (VV) and Vertically emitted and Horizontally received (VH) polarisation channels, from Sentinel-1, soil moisture, electrical conductivity, pH, temperature and SOC from the laboratory-based testing methods were used as regression parameters. The RF regression gave a Root Mean Square Error (RMSE) of 0.78 and R2 statistics of 0.887, while the OLS method performed better with an RMSE of 0.53 and an R2 value of 0.907. It was also observed that the backscatter from VV and VH polarisation channels, when used synergistically with field data, have the highest Feature Importance (FI) score in both RF and OLS regression models for SOC estimation.